Journal of Visualized Experiments

Stereotaxic surgical approach to microinject the caudal brainstem and upper cervical spinal cord via the cisterna magna in mice

--Manuscript Draft--

Article Type:	Methods Article - JoVE Produced Video
Manuscript Number:	JoVE63344R3
Full Title:	Stereotaxic surgical approach to microinject the caudal brainstem and upper cervical spinal cord via the cisterna magna in mice
Corresponding Author:	Veronique VanderHorst UNITED STATES
Corresponding Author's Institution:	
Corresponding Author E-Mail:	vvanderh@bidmc.harvard.edu
Order of Authors:	Krutika Joshi, Ph.D.
	Alana Kirby
	Jianguo Niu
	Veronique VanderHorst
Additional Information:	
Question	**Response**
Please specify the section of the submitted manuscript.	Neuroscience
Please indicate whether this article will be Standard Access or Open Access.	Standard Access ($1400)
Please indicate the **city, state/province, and country** where this article will be **filmed**. Please do not use abbreviations.	Boston, Massachusetts, United States of America
Please confirm that you have read and agree to the terms and conditions of the author license agreement that applies below:	I agree to the Author License Agreement
Please confirm that you have read and agree to the terms and conditions of the video release that applies below:	I agree to the Video Release
Please provide any comments to the journal here.	

TITLE:

Stereotaxic Surgical Approach to Microinject the Caudal Brainstem and Upper Cervical Spinal Cord *via* the Cisterna Magna in Mice

AUTHORS AND AFFILIATIONS:

Krutika Joshi, Alana Kirby, Jianguo Niu, Veronique VanderHorst

Beth Israel Deaconess Medical Center, Harvard Medical School, Boston, USA

Email addresses of co-authors:

Krutika Joshi (kjoshi@bidmc.harvard.edu)
Alana Kirby (Alana_E_Kirby@rush.edu)
Jianguo Niu (niujg2008@hotmail.com)

Corresponding author:

Veronique VanderHorst (vvanderh@bidmc.harvard.edu)

SUMMARY:

Stereotaxic surgery to target brain sites in mice commonly involves access through the skull bones and is guided by skull landmarks. Here we outline an alternative stereotaxic approach to target the caudal brainstem and upper cervical spinal cord *via* the cisterna magna that relies on direct visualization of brainstem landmarks.

ABSTRACT:

Stereotaxic surgery to target brain sites in mice is commonly guided by skull landmarks. Access is then obtained *via* burr holes drilled through the skull. This standard approach can be challenging for targets in the caudal brainstem and upper cervical cord due to specific anatomical challenges as these sites are remote from skull landmarks, leading to imprecision. Here we outline an alternative stereotaxic approach *via* the cisterna magna that has been used to target discrete regions of interest in the caudal brainstem and upper cervical cord. The cisterna magna extends from the occipital bone to the atlas (i.e., the second vertebral bone), is filled with cerebrospinal fluid, and is covered by dura mater. This approach provides a reproducible route of access to select central nervous system (CNS) structures that are otherwise hard to reach due to anatomical barriers. Furthermore, it allows for direct visualization of brainstem landmarks in close proximity to the target sites, increasing accuracy when delivering small injection volumes to restricted regions of interest in the caudal brainstem and upper cervical cord. Finally, this approach avoids the cerebellum, which can be important for motor and sensorimotor studies.

INTRODUCTION:

Standard stereotaxic surgery to target brain sites in mice[1] commonly involves fixation of the skull using a set of ear bars and a mouth bar. Coordinates are then estimated based on reference atlases[2,3], and skull landmarks, namely, bregma (the point where the sutures of the frontal and parietal bones come together) or lambda (the point where the sutures of the

parietal and occipital bones come together; **Figure 1A,B**). Through a burr hole into the skull above the estimated target, the target region can then be reached, either for delivery of microinjections or instrumentation with cannulas or optic fibers. Due to variation in the anatomy of these sutures and errors in the localization of bregma or lambda[4,5], the position of zero points in relation to the brain varies from animal to animal. While small errors in targeting, that result from this variability, are not a problem for large or nearby targets, their impact is greater for smaller areas of interest that are remote from the zero points in the anteroposterior or dorsoventral planes and/or when studying animals of varying size due to age, strain and/or sex. There are several additional challenges that are unique for the medulla oblongata and the upper cervical cord. First, small changes in anteroposterior coordinates are associated with significant changes in dorsoventral coordinates relative to the dura, due to the position and shape of the cerebellum (**Figure 1Bi**)[2,6,7]. Second, the upper cervical cord is not contained within the skull[2]. Third, the slanting position of the occipital bone and overlying layer of neck muscles[2] makes the standard stereotaxic approach even more challenging for structures located near the transition between the brainstem and spinal cord (**Figure 1Bi**). Finally, many targets of interest in the caudal brainstem and cervical cord are small[2], requiring precise and reproducible injections[8,9].

An alternative approach through the cisterna magna circumvents these problems. The cisterna magna is a large space that extends from the occipital bone to the atlas (**Figure 1A**, i.e., the second vertebral bone)[10]. It is filled with cerebrospinal fluid and covered by dura mater[10]. This space between the occipital bone and the atlas opens when anteroflexing the head. It can be accessed by navigating in between the overlying paired bellies of the longus capitis muscle, exposing the dorsal surface of the caudal brainstem. Regions of interest can then be targeted based upon the landmarks of these regions themselves if they are located near the dorsal surface; or by using the obex, the point where the central canal opens into the IV ventricle, as a zero point for coordinates to reach deeper structures. This approach has been successfully used in a variety of species, including the rat[11], cat[12], mouse[8,9], and non-human primate[13] to target the ventral respiratory group, medullary medial reticular formation, the nucleus of the solitary tract, area postrema, or hypoglossal nucleus. However, this approach is not widely utilized as it requires knowledge of anatomy, a specialized toolkit, and more advanced surgical skills compared to the standard stereotaxic approach.

Here we describe a step-by-step surgical approach to reach the brainstem and upper cervical cord *via* the cisterna magna, visualize landmarks, set the zero point (**Figure 2**), and estimate and optimize target coordinates for stereotaxic delivery of microinjections into the discrete brainstem and spinal cord regions of interest (**Figure 3**). We then discuss the advantages and disadvantages related to this approach.

PROTOCOL:

The author declares that the protocol follows the guidelines of the Institutional Animal Care and Use Committee at Beth Israel Deaconess Medical Center.

1. Preparation of surgical instruments and stereotaxic frame

NOTE: The surgery is performed under aseptic conditions.

1.1. Install the stereotaxic arm with a micropipette or syringe filled with an injectable of choice (adeno-associated virus (AAV) or conventional tracer) on the stereotaxic frame and prepare the mouse adapter (**Figure 2A**).

1.2. Prepare autoclaved surgical instruments (**Table of materials**) and place them on a sterile surface.

2. Anesthesia induction and mouse preparation

2.1. Turn on O_2 at 0.5 L/min and set the isoflurane vaporizer at 4.0, making sure that O_2 flow is to the induction box.

CAUTION: Make sure that the isoflurane induction box is placed in a hood and that the isoflurane is scavenged away from the surgical site.

2.2. Place the mouse (10-week-old male C57BL/6J) in the induction chamber.

2.3. Once breathing has slowed, open the induction chamber, and lift the mouse slightly. Use clippers to remove hair from head to shoulders.

3. Positioning of the mouse in the stereotaxic frame

3.1. Move the mouse to the stereotaxic frame and place the nose in a flexible nose cone. At this stage, make sure the O_2 flow is now directed to the nose cone.

3.2. Place the mouse in the stereotaxic frame using ear bars only.

NOTE: Make sure the ear bars are even and the head is level.

3.3. Anteroflex the head of the mouse to a 90° angle by manually guiding the nose. To secure this position, place a plastic barrier between the ear bar pillars of the mouse adapter, parallel to the pillars. The flat part of the skull serves as the reference, similar to the flat skull approach in conventional stereotaxic surgery.

NOTE: Do not over flex the head as this impedes airflow through the upper airway.

3.4. Place the heating pad underneath the mouse, and then make sure that the neck and the rest of the body are positioned at the same level (i.e., at approximately 180° or parallel to the table). The toolbox that holds the spring scissors can be used to lift the body to this position.

NOTE: This step is important as the caudal brainstem and upper cervical cord move depending on position, in contrast to more rostral parts of the CNS which are held in place by the skull.

3.5. Inject a single dose of 4 mg/kg Meloxicam slow-release (SR) subcutaneously (s.c.) at a volume of 2 µL/g body weight and place lubricant on the eyes.

3.6. Clean the surgical incision site first with a 70% alcohol prep pad, then with a betadine prep pad, and then again with an alcohol prep pad and let dry.

3.7. Place a drape underneath the body.

3.8. Disinfect hands and put on sterile gloves.

3.9. Place a drape at the surgical site.

4. Surgery to access the cisterna magna

4.1. Make sure the mouse is appropriately anesthetized by pinching the toes or checking the corneal reflex.

4.2. Reduce isoflurane to maintenance levels (2.0).

4.3. Make a 1–1.2 cm incision with surgical blade #10 from the edge of the occipital bone toward the shoulders in one smooth movement.

4.4. Make an incision in the midline raphe of the trapezius muscle. This exposes the paired longus capitis muscles.

NOTE: In mice, the trapezius muscle is a very thin, almost transparent muscle. Make sure to stay in the midline and do not cut into the underlying muscles as this will cause unnecessary bleeding.

4.5. Place both retractor hooks in between the paired longus capitis muscles, one oriented to the left and the other to the right. The weight of the hemostats provides tension to the retractor hooks which can be modified by re-adjusting the position of the hemostats.

4.6. Position the surgical microscope in place to better visualize the surgical field.

4.7. Use the blunt laminectomy forceps to separate the left and right bellies of the paired longus capitis muscle, starting from the occiput, where the midline is readily visible. Guide the blunt forceps across the bone of the occiput in the midline down to where it meets the cisternal dura mater, and then continue across the dura mater to the atlas.

NOTE: There is no need to cut through the paired longus capitis muscles as nothing holds them

together in the midline; doing so will cause unnecessary bleeding.

4.8. Reposition the retractors and adjust the tension by repositioning the hemostats, opening the view of the cisterna magna.

4.9. Use the blunt laminectomy forceps to separate the muscles further in the midline to get a good viewing window of the brainstem and cerebellum.

4.10. Repeat steps 4.7–4.9 as needed until the cerebellum and brainstem come in view below the dura.

4.11. Using blunt laminectomy forceps, clear the dura of the small strands of connective tissue by moving the forceps from the midline in a lateral direction, until there is a clear view of the brainstem and to create more lateral space, as needed for the target.

5. Opening of the cisternal membrane

5.1. Use the angled Dumont forceps (#4/45) to grab the dura, which extends from the occipital bone to the atlas. Grab the dura near the occipital bone and use the spring scissors to make a small opening (~0.5 to 1.5 mm) in the dura.

NOTE: At this rostral location, the space between the brainstem and the overlying dura is widest, providing ample room for safe manipulation of the dura.

5.2. Use the spring scissors to lift the dura and open the dura further. The size of the window depends on the target.

NOTE: A larger window will be needed when making multiple longitudinal injections or bilateral injections; a small window will be sufficient when making single unilateral or midline injections.

5.3. Once the dura is opened, drain excess cerebrospinal fluid with a sterile cue tip.

6. Identification of landmarks and zero point

6.1. View the dorsal surface of the brainstem with detailed landmarks through the open dura. The obex, the point where the central canal opens into the IV ventricle, is the standard anterior-posterior and mediolateral zero point.

7. Target coordinates

NOTE: For various targets, we have included a list of standard coordinates with anterior posterior (AP) and mediolateral (ML) coordinates relative to zero-point bregma and cisterna magna coordinates with AP and ML coordinates relative to zero point obex to facilitate the transition between methodologies (**Table 1**). Dorsoventral (DV) coordinates are relative to the

surface of the brain or cerebellum (standard approach) or the surface of the brainstem or upper cervical cord (cisterna magna approach) at the point of AP and ML entry. Planning should be done prior to surgery.

7.1. Use the three sets of coordinates to determine the target: AP, ML, and DV. Due to the head position, the relative orientation of brainstem structures varies by location.

7.1.1. For target distance >0.4 mm from caudal to the obex (**Figure 1B**, green) perform the following.

7.1.1.1. AP: Use any standard stereotaxic reference atlas (e.g., Paxinos and Franklin atlas[2]) or tissue series cut in the transverse plane to estimate the AP distance between obex and the target.

7.1.1.2. ML: Use any standard stereotaxic reference atlas or tissue series cut in the transverse plane to estimate the ML distance between obex and the target.

7.1.1.3. DV: Estimate coordinates relative to the surface of the brain or cerebellum at the AP and ML target point. Use any standard stereotaxic reference atlas or tissue series cut in the transverse plane to estimate the distance between the brainstem surface at the desired AP and ML coordinates and the target.

7.1.2. For target distance <0.4 mm from caudal to the obex (**Figure 1B**, orange) perform the following.

7.1.2.1. AP: Adjust coordinates to account for anteroflexion of the brainstem. For ventral and rostral coordinates, the AP brainstem entry point will be more caudal relative to the target AP coordinate in the standard plane.

7.1.2.2. ML: Derive target coordinates from a standard stereotaxic reference atlas or tissue series cut in the transverse plane. Coordinates will be relative to the visualized midline at the target AP level.

7.1.2.3. DV: Estimate coordinates relative to the surface of the brainstem at the AP and ML target point. Adjust DV to account for anteroflexion of the brainstem. For ventral and rostral coordinates, the DV coordinates will be larger than the distance from the dorsal surface of the brainstem in the standard plane.

8. Injection of the target

8.1. Lower the pipette or syringe to the target using the stereotaxic arm and inject solution as for standard stereotaxic approaches. Leave in place for 1–5 min after injection, to avoid a needle track when using volumes between 3–50 nL. Then, lift the pipette or syringe using the stereotaxic arm.

8.2. Repeat step 8.1. for multiple targets.

9. Closure of the surgical field

9.1. Remove the hooks carefully from the surgical field. The paired longus capitis muscles will fall back into a neutral position, fully covering the cisterna magna. Do not close the trapezius muscle and dura mater in the midline as they are too fragile to hold sutures.

9.2. Close the skin with three nylon or polypropylene sutures (5-0 or 6-0).

10. Post-operative care

10.1. Turn off isoflurane and remove the mouse from the stereotaxic frame. Place the mouse in a clean cage on a heating pad and observe until awake and moving.

10.2. Monitor health status, weight, and sutures on post-operative days 1–3. Remove sutures on day 10 if not already removed.

REPRESENTATIVE RESULTS:

The cisterna magna approach makes it possible to target caudal brainstem and upper cervical cord structures that are otherwise hard to reach *via* standard stereotaxic approaches or are prone to inconsistent targeting. The surgery to reach the cisterna magna requires incisions of the skin, a thin layer of trapezius muscle, and opening of the dura mater and is therefore well tolerated by mice. It is especially efficient and less invasive when targeting multiple (longitudinally dispersed or bilateral) sites, as it does not require drilling of multiple burr holes as in standard stereotaxic approaches. In mice, we have routinely targeted structures such as the hypoglossal nucleus[9], ventral respiratory group[8], and adjacent reticular formation[8] in the caudal brainstem using the cisterna magna approach, as we further illustrate for the hypoglossal nucleus and the ventromedial medulla (GiV) in **Figure 3**. For example, the hypoglossal nucleus is a slim but rostrocaudally elongated column of motoneurons in the dorsal medulla oblongata and its rostral pole can be targeted *via* a standard approach. However, as the DV coordinates (~4.5 mm) are mostly dictated by the overlying cerebellum with only 1.2–1.4 mm entering the brainstem, a relatively small difference in positioning of the head of the mouse could therefore easily result in a misplaced injection. Due to the proximity of this target to the zero-point obex, it can be more reliably targeted *via* the cisterna magna approach. Furthermore, the caudal end of the hypoglossal nucleus which extends until the transition between the brainstem and spinal cord can be targeted by the same cisterna magna approach, whereas the standard approach would have to be modified to reach such a caudal site by angling the AP approach and adjusting coordinates to avoid the occipital bone and overlying neck musculature.

In order to determine the accuracy of the cisterna magna approach versus the standard approach, we measured the distance between intended and actual target sites in the

anteroposterior, mediolateral, and dorsoventral planes for ventral (ventromedial medulla; GiA/V; N = 10) and dorsal (NuXII; N = 16) regions. The measurements were made in transverse sections of the caudal brainstem (**Figure 3**). The results (**Figure 4**) show significantly smaller errors in the anteroposterior, mediolateral, and especially dorsoventral planes for the cisterna magna approach compared to the standard approach. These results highlight the enhanced accuracy of the cisterna magna approach for these targets. We have included standard stereotaxic coordinates (relative to bregma, derived from Paxinos and Franklin [2], but optimized for our studies) and cisterna magna coordinates (relative to the obex) in **Table 1**. These coordinates have all been optimized and verified as shown for the hypoglossal nucleus and ventromedial medulla in **Figure 3**.

FIGURE AND TABLE LEGENDS:

Figure 1: Schematic representation of key landmarks, target areas, and the plane of the stereotaxic cisterna magna approach. (**A**) Key anatomical landmarks and positioning in the sagittal plane. (**B**) Areas that can be reached through the standard stereotaxic approach versus cisterna magna stereotaxic approach and relation to their reference points. i) The standard approach makes use of bony landmarks bregma and lambda, which are distant from target regions in magenta and purple. The area in magenta (caudal medulla oblongata and upper cervical cord) is challenging to reach due to the slanting occipital bone and neck muscles. The area in purple (rostral medulla oblongata) is prone to movement and distant from traditional landmarks. ii) The cisterna magna approach is appropriate for accessing the caudal medulla oblongata and upper cervical cord and has advantages when studying brainstem structures that are organized into longitudinal columns that extend from the caudal medulla oblongata rostrally, up to the level of the caudal pons. (**C**) Schematic of the planes of various stereotaxic reference atlases in relation to the cisterna magna approach.

Figure 2: Step-by-step schematic overview of the stereotaxic cisterna magna approach. (**A**) Mouse adapter with ear bars evenly positioned at the highest level, the mouth bar at a lowered position, and a plastic card to secure the anteroflexed head at a 90° angle. (**B**) Secure the mouse into the stereotacxic frame using the ear bars and anteroflex the head at 90° and keep in position *via* a rigid plastic card, with the stereotaxic frame as a reference. (**C**) Make sure the body is elevated so it is in the same plane as the occiput. Palpate key landmarks. (**D**) Make a skin incision from the occiput to the rostral part of the shoulders. (**E**) Make an incision in the raphe of the trapezius muscle. Make sure to stay in the midline and do not cut into the underlying muscles. (**F**) Identify the midline between the two bellies of the longus capitis muscle, starting at the occiput, and guide the laminectomy forceps in a caudal direction. (**G**) Place each of the wound hooks in between the bellies of the longus capitis muscle and re-position until the cisterna magna comes in view. (**H**) Identify bony landmarks (occipital bone, atlas), the dura mater that extends between these bony structures, and the underlying cerebellum and brainstem. Clean the dura mater as needed to expose the target level. (**I**) Using spring scissors and fine forceps open the dura. (**J**) Identify the obex, which forms the AP and ML zero point. Move the pipette to the AP and ML coordinates of choice. Lower the pipette until it reaches the dorsal surface of the brainstem. This is the DV zero point. Lower the pipette to the desired coordinate. (**K**) Remove the pipette and the wound hooks and let the longus capitis

muscles resume their original position. (**L**) Close the wound and remove the mouse from the stereotaxic frame.

Figure 3: Evaluation of target coordinates. Low magnification photomicrographs of the caudal brainstem. (**A**) Injection of retrograde tracer cholera toxin subunit b (CTb; blue) into the hypoglossal nucleus of a ChAT-cre L10 GFP (green) reporter mouse (female, 6 months old). Note that the CTb injection is restricted to the hypoglossal nucleus. (**B**) Transfection of glutamatergic cells of a vGluT2-ires-cre L10 GFP reporter (green) mouse (male, 2 months old) with a conditional anterograde tracer (magenta) in the ventral part of the caudal medial medulla oblongata (caudal pole of the GiV region). (**C**) Conditional retrograde tracing in a vGLuT2-ires-cre mouse (male, 2 months old) showing TVA (magenta) transfection of glutamatergic neurons and modified rabies infection (green) in the caudal medial medulla oblongata (caudal pole of the GiV region). Rabies virus was injected into the upper cervical spinal cord. Internal landmarks serve as a guidance. Abbreviations—cAmb: Compact Nucleus of the Ambiguus complex; Ap: Area Postrema; DMV: Dorsal Motor Nucleus of the Vagus; GiV: Gigantocellular Nucleus, ventral part; IO: Inferior Olive; IRt: Intermediate Reticular Nucleus; LRN: Lateral Reticular Nucleus; NuXII- Hypoglossal Nucleus; sol: Nucleus of the Solitary Tract; Sp5: Spinal Trigeminal Nucleus; VRG: ventral respiratory group. Scale bar: 200 µm.

Figure 4: Comparison of the accuracy between the standard and cisterna magna approaches. Mean distance between the center of the intended target and the center of the actual site in the anteroposterior plane (**A**), mediolateral plane (**B**), and dorsoventral plane (**C**). Data was obtained from N = 13 adult mice using a standard approach and N = 13 adult mice using a cisterna magna approach. The radius of the target was set at 30 µm. The results show higher accuracy in the anteroposterior plane ($t(24) = 2.08$, $p = 0.049$; two-tailed *t*-test; alpha 0.05), mediolateral plane ($t(24) = 2.55$, $p = 0.018$; two-tailed *t*-test; alpha 0.05) and dorsoventral plane ($t(24) = 4.33$, $p = 0.0002$; two-tailed *t*-test; alpha 0.05). Bar graphs represent the mean with standard deviation and individual dots represent values in each mouse.

Table 1: Overview of standard and cisterna magna stereotaxic coordinates to target caudal brainstem structures. Please note that for both the standard and cisterna magna approaches, coordinates from the Paxinos and Franklin atlas[2] have been adjusted until regions of interest were appropriately targeted as verified by histology (**Figure 3**). Also, note that areas in the reticular formation lack well-defined boundaries and are here labeled as in Paxinos and Franklin[2]. Abbreviations—AP: anteroposterior. ML: mediolateral. DV: dorsoventral. ChAT: Choline Acetyltransferase; F: Female; M: Male; M&F: Male and Female; NA: not applicable; Pet1: plasmacytoma expressed transcription factor 1; Sert: Serotonin transporter, vGaT: Vesicular GABA transporter; vGluT2: Vesicular Glutamate transporter 2; WT: Wild type. All coordinates are in millimeter (mm).

DISCUSSION:

Standard stereotaxic surgery commonly relies on skull landmarks to calculate the coordinates of target sites in the CNS[1]. Target sites are then accessed *via* burr holes that are drilled through the skull[1]. This method is not ideal for the caudal brainstem as target sites are located distant

from the skull landmarks in the anteroposterior and dorsoventral planes[2] and as the anatomy of the skull and overlying muscles make access challenging[6] (**Figure 1Bi**). Our study describes an alternate stereotaxic approach for accessing target sites in the caudal brainstem and upper spinal cord called the cisterna magna approach. Key features that make this method different from a standard stereotactic approach are positioning, with anteroflexion of the head to open up the cisterna magna, and use of key brainstem landmarks at the dorsal surface of the brainstem as reference points such as the obex. Our results indicate that this approach is suitable for the delivery of small volumes (5–50 nL) of tracers or adeno-associated viruses (AAVs) into discrete brainstem structures. Furthermore, the use of a reference point that represents a CNS landmark, rather than a bony structure, and that is in close proximity to the intended target increases reproducibility and accuracy for small targets and small injection volumes, as relevant for circuit mapping and chemogenetic studies (**Figure 3**)[14,15].

As with any protocol, the cisterna magna approach has steps that are critical in order to achieve reproducibility. As with any stereotaxic approach which is dependent on coordinates in three different planes (anteroposterior, mediolateral, and dorsoventral), positioning is critical. For the cisterna magna approach, this involves not only the position of the head, which should be anteroflexed at 90° but also that of the body, which should be elevated so that the caudal brainstem and upper cervical cord are in the same plane. Another critical step is to avoid unnecessary manipulations that cause bleeding, as this would hamper the visualization of key landmarks. There are two manipulations that carry a high risk of bleeding. Firstly, the dura mater covering the cisterna magna is covered by a relatively large muscle (longus capitis). As this is a paired muscle, with one belly on either side of the midline, the two bellies of this muscle will only need to be gently separated in the midline. Incision of these muscles is not necessary and will cause bleeding. Secondly, on the successful opening of the dura mater, a variable number of veins with a variable course will become visible on top of the dorsal surface of the caudal brainstem and upper cervical cord. These veins should be avoided by applying minor adjustments in coordinates (up to 0.1 mm) or, if the experimental paradigm allows, by selecting a different target.

A major advantage of the cisterna magna approach is that it provides access to the brainstem and upper cervical structures that are challenging to reach when using the standard stereotaxic plane as they are located near the caudal end of or just caudal to the occipital bone. Furthermore, the approach avoids the cerebellum and therefore cerebellar lesion effects or spurious labeling *via* a needle tract, which can affect study outcomes when using standard methodology are not a concern. Another advantage of the cisterna magna approach is that the dorsal surface of the brainstem becomes visible. This provides the opportunity to use a landmark on the dorsal surface as a reference point for coordinates. Furthermore, the approach is flexible and can be optimized depending on the target. For example, we used a midline landmark, the obex, as the reference point. However, when targeting dorsal structures, the structure of interest itself may dictate the landscape of the dorsal surface. For example, the external cuneate nucleus protrudes dorsally, and can thus be visualized and injected directly. For lateral targets, such as the ventral respiratory group or ambiguous complex, the cisterna magna window can be increased in a lateral direction. Likewise, for targeting of upper cervical

structures, the window can be extended towards the atlas. While we used a mouse adaptor placed in a large animal stereotactic frame, the approach can easily be adapted to other frames or setups, as long as the key steps are being followed. For example, instead of a plastic card, the mouth bar can be placed against the bridge of the nose to keep the head in a stable anteroflexed position. It is worth noting that coordinates of brainstem target sites with the obex as zero point, as provided in **Table 1**, serve as a reference, and adjustments may be indicated based upon the mouse strain, age, sex, calibration of the stereotaxic arm, and positioning technique, similar to adjustments that one needs to make when deriving target coordinates for a standard approach from a reference atlas. This requires insight into the plane of the approach, especially for more rostral targets as illustrated in **Figure 1**. Testing of coordinates can be done by using different tracers, for example, fluorescent beads or fluorescent-tagged Cholera Toxin subunit b for different coordinates in the same mouse. Histological analyses of brainstem/spinal tissue sections (not covered in this protocol) then provide feedback about localization relative to objective internal landmarks[8,9,11,16] or for comparison with a reference atlas. Coordinates can then be adjusted, tested again, and finalized.

The cisterna magna approach also has limitations. CNS regions that can be reached *via* this approach are restricted to the caudal pons, medulla oblongata, and upper cervical cord. While the caudal pons can be accessed easily *via* the standard approach, the cisterna magna approach has advantages when studying subdivisions of longitudinally oriented structures that extend from the medulla oblongata into the caudal pons, as is the case for subdivisions within the reticular formation. Another relative limitation occurs when using this approach for the second time in the same mouse, for example, in modified rabies tracing[14]. The presence of scar tissue may increase the duration of the surgery or obscure minor landmarks. However, in our hands, this method has still been superior to the standard stereotaxic approach in this case, as the site of the first injection can be documented in relation to the position of veins of other unique landmarks, making it easy to find the exact entry point back. While this approach is superior for tracing studies in the caudal medulla and upper spinal cord, it cannot be used to chronically implant hardware. Therefore, for *in-vivo* optogenetics and calcium imaging studies that require implantation of optic fibers[17] the cisterna magna approach can be used first to deliver an AAV to the target site, followed by a second surgery using a standard approach to instrument mice with fibers or cannulas. This approach enables one to keep the target site discrete, while fiber/hardware placement is more forgiving (i.e., can be less accurate), due to the relatively large size of the hardware. Lastly, the cisterna magna approach requires more advanced surgical skills than a standard stereotaxic approach. Rather than recognition of simple bony landmarks, it requires insight into more complex brainstem and musculoskeletal landmarks. Also, as with any delicate surgery, the success and efficiency of the procedure depend on a proper toolkit that is in excellent condition. This protocol addresses the latter issues and can be used as a detailed guide by experimenters.

In conclusion, the cisterna magna approach is complementary to the standard stereotaxic approach and provides multiple advantages when targeting the caudal brainstem and upper cervical cord, which are not easily accessed *via* a standard stereotaxic approach. It uses

reference points that are CNS rather than bony landmarks which are in close proximity to the intended targets, increasing reproducibility and accuracy. This makes the approach especially valuable when small injection volumes need to be delivered to discrete sites in the context of detailed mapping or chemogenetic studies. This approach is also relevant for functional chemogenetic, optogenetic, fiber photometry, or lesion approaches, where an AAV virus or toxin is delivered to a target with motor function or sensorimotor integration as a readout, as this method avoids a course through the cerebellum and therefore limits its interference in study results. From an animal welfare point of view, the procedure does not require drilling multiple burr holes to access sites bilaterally or longitudinally, reducing the duration of the surgery and invasiveness of the procedure. While we outlined the approach in detail for mice, the same principles apply to other species[11–13].

ACKNOWLEDGMENTS:

This work was supported by R01 NS079623, P01 HL149630, and P01 HL095491.

DISCLOSURES:

The authors have nothing to disclose.

REFERENCES:

1. Rodent Stereotaxic Surgery. *JoVE Science Education Database*. **Neuroscience** (2021).
2. Paxinos, G., Franklin, K. B. J. *The Mouse Brain in Stereotaxic Coordinates*. Academic Press (2001).
3. Lein, E. S. et al. Genome-wide atlas of gene expression in the adult mouse brain. *Nature*. **445** (7124), 168–176 (2007).
4. Rangarajan, J. R. et al. Image-based in vivo assessment of targeting accuracy of stereotactic brain surgery in experimental rodent models. *Scientific Reports*. **6** (1), 38058 (2016).
5. Blasiak, T., Czubak, W., Ignaciak, A., Lewandowski, M. H. A new approach to detection of the bregma point on the rat skull. *Journal of Neuroscience Methods*. **185** (2), 199–203 (2010).
6. Popesko, P., Rajtova, V., Horak, J. *A Colour Atlas of the Anatomy of Small Laboratory Animals, Volume 2: Rat, Mouse and Golden Hamster*. Wolfe Publishing Ltd. **2** (1992).
7. Allen Mouse Brain Atlas. *Allen Institute for Brain Science*. at <https://mouse.brain-map.org/experiment/thumbnails/100042147?image_type=atlas> (2004).
8. Vanderhorst, V. G. J. M. Nucleus retroambiguus-spinal pathway in the mouse: Localization, gender differences, and effects of estrogen treatment. *The Journal of Comparative Neurology*. **488** (2), 180–200 (2005).
9. Yokota, S., Kaur, S., VanderHorst, V. G., Saper, C. B., Chamberlin, N. L. Respiratory-related outputs of glutamatergic, hypercapnia-responsive parabrachial neurons in mice. *Journal of Comparative Neurology*. **523** (6), 907–920 (2015).
10. Anselmi, C. et al. Ultrasonographic anatomy of the atlanto-occipital region and ultrasound-guided cerebrospinal fluid collection in rabbits (Oryctolagus cuniculus). *Veterinary Radiology & Ultrasound*. **59** (2), 188–197 (2018).
11. Herbert, H., Moga, M. M., Saper, C. B. Connections of the parabrachial nucleus with the nucleus of the solitary tract and the medullary reticular formation in the rat. *The Journal of*

Comparative Neurology. **293** (4), 540–580 (1990).
12. Vanderhorst, V. G., Holstege, G. Caudal medullary pathways to lumbosacral motoneuronal cell groups in the cat: evidence for direct projections possibly representing the final common pathway for lordosis. *The Journal of Comparative Neurology*. **359** (3), 457–475 (1995).
13. Vanderhorst, V. G., Terasawa, E., Ralston, H. J., Holstege, G. Monosynaptic projections from the nucleus retroambiguus to motoneurons supplying the abdominal wall, axial, hindlimb, and pelvic floor muscles in the female rhesus monkey. *The Journal of Comparative Neurology*. **424** (2), 233–250 (2000).
14. Wall, N. R., Wickersham, I. R., Cetin, A., De La Parra, M., Callaway, E. M. Monosynaptic circuit tracing in vivo through Cre-dependent targeting and complementation of modified rabies virus. *Proceedings of the National Academy of Sciences of the United States of America*. **107** (50), 21848–21853 (2010).
15. Krashes, M. J. et al. Rapid, reversible activation of AgRP neurons drives feeding behavior in mice. *The Journal of Clinical Investigation*. **121** (4), 1424–1428 (2011).
16. Ganchrow, D. et al. Nucleus of the solitary tract in the C57BL/6J mouse: Subnuclear parcellation, chorda tympani nerve projections, and brainstem connections. *The Journal of Comparative Neurology*. **522** (7), 1565–1596 (2014).
17. Ung, K., Arenkiel, B. R. Fiber-optic implantation for chronic optogenetic stimulation of brain tissue. *Journal of Visualized Experiments: JoVE*. (68), 50004 (2012).

Figure 1

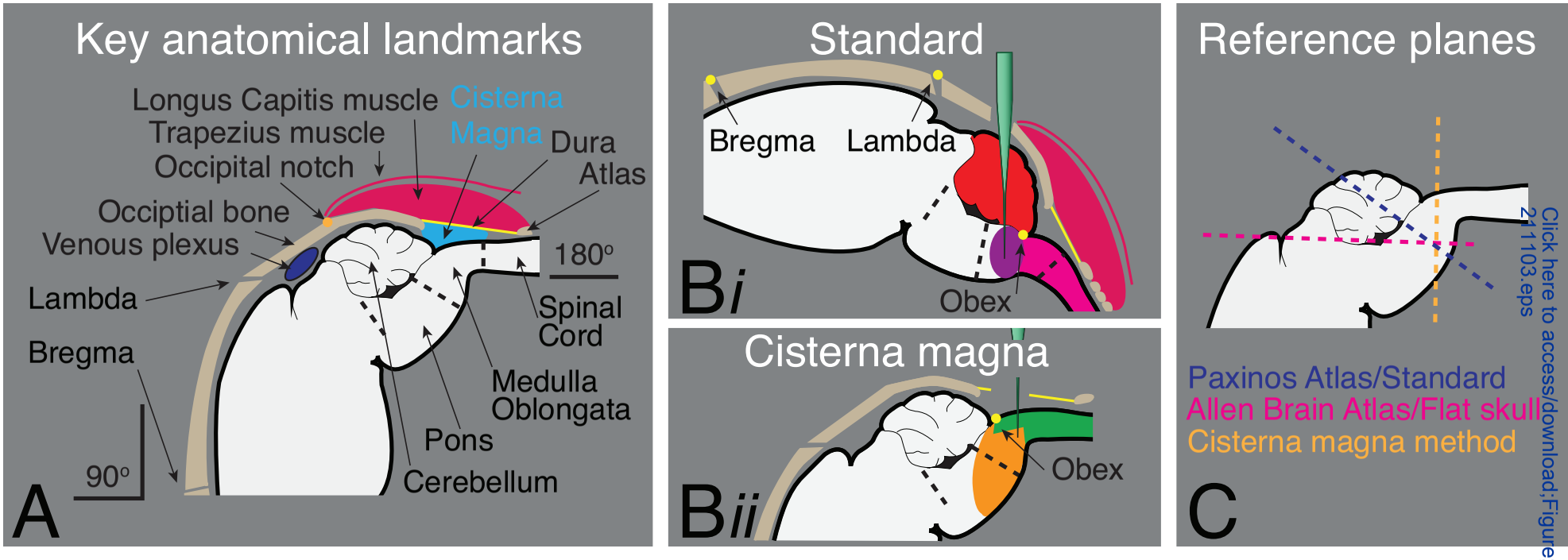

Figure 2

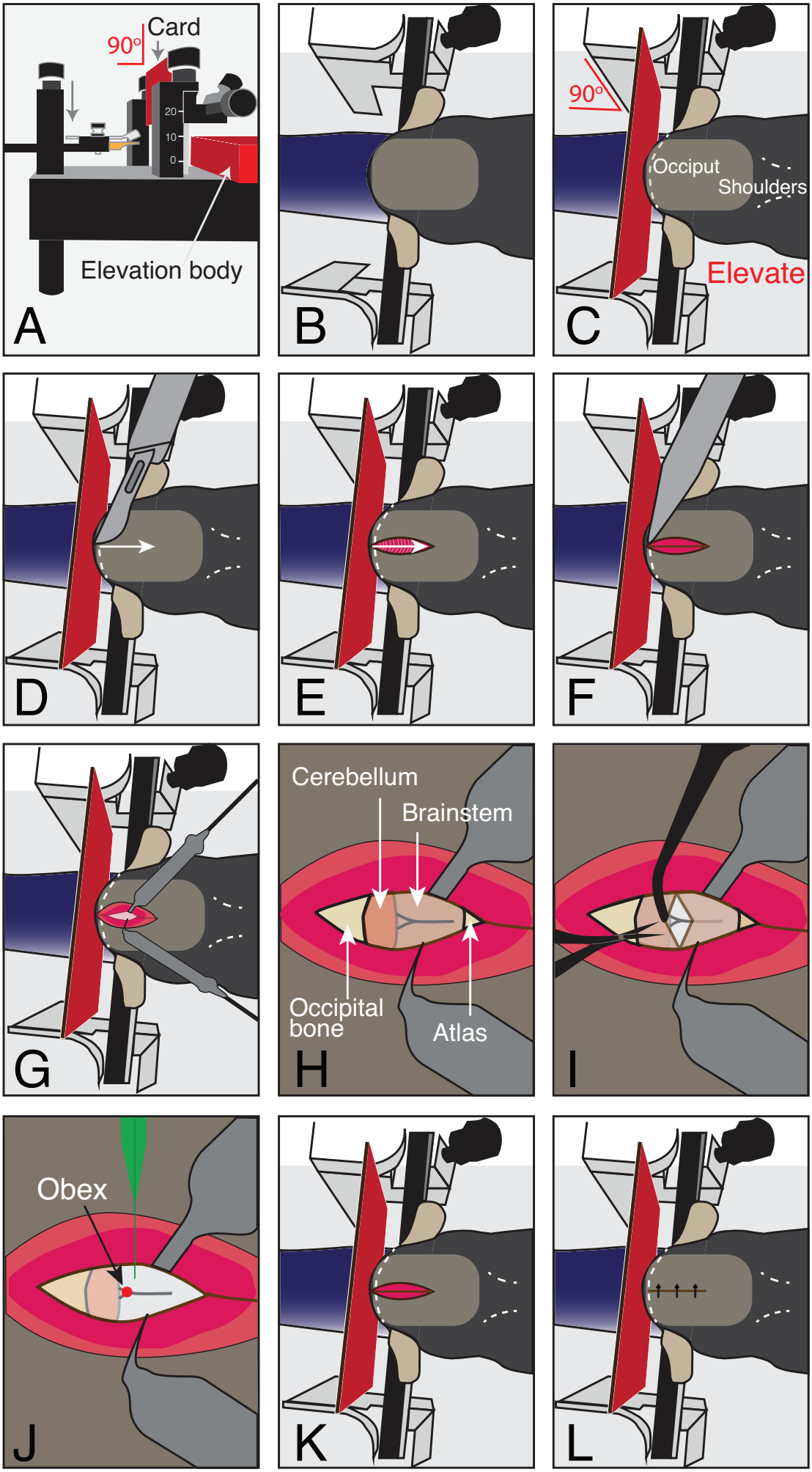

Figure 3- Evaluation of Target Coordinates

Click here to access/download;Figure;Figure 3 - Flattened downsampled 300.jpg

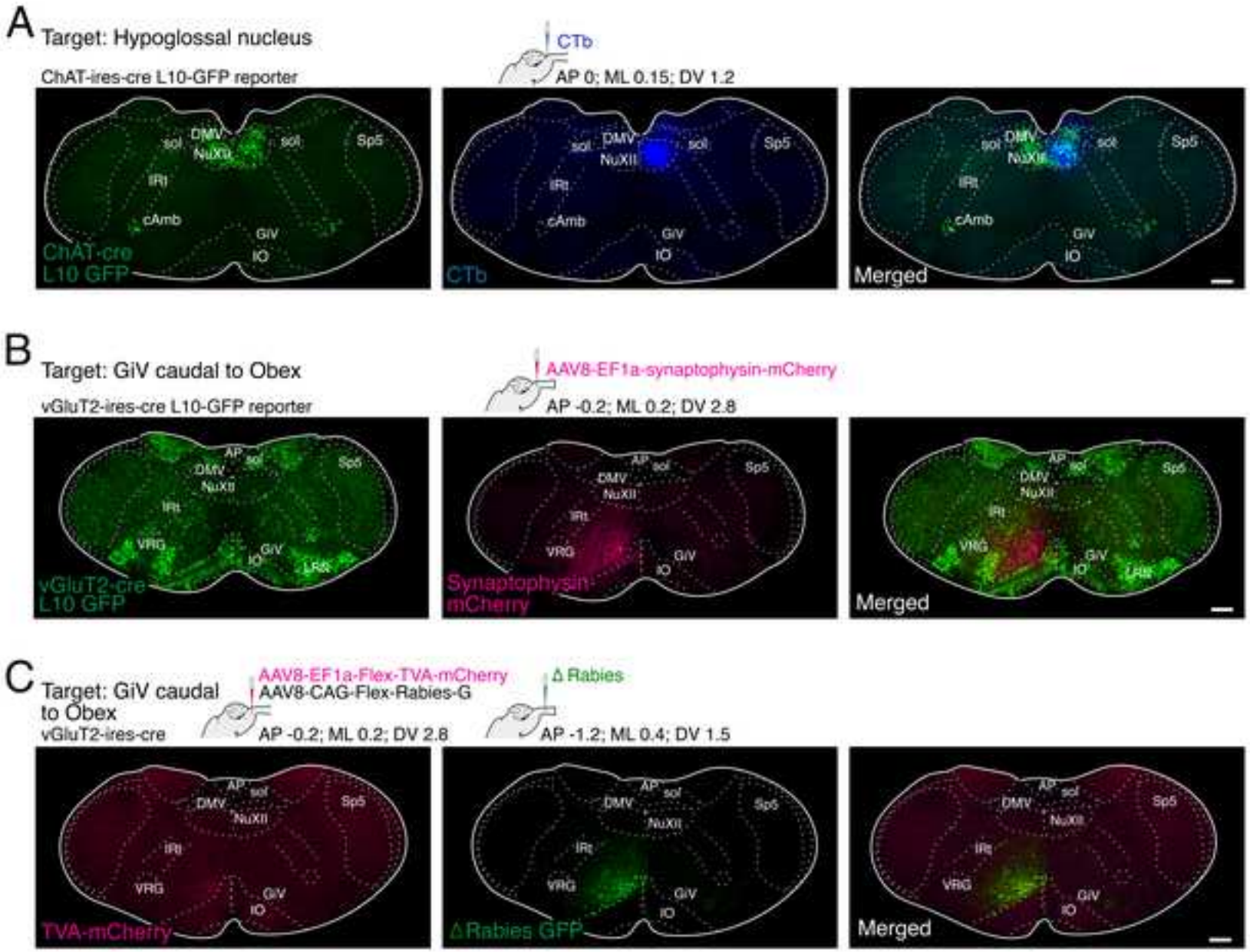

Figure 4

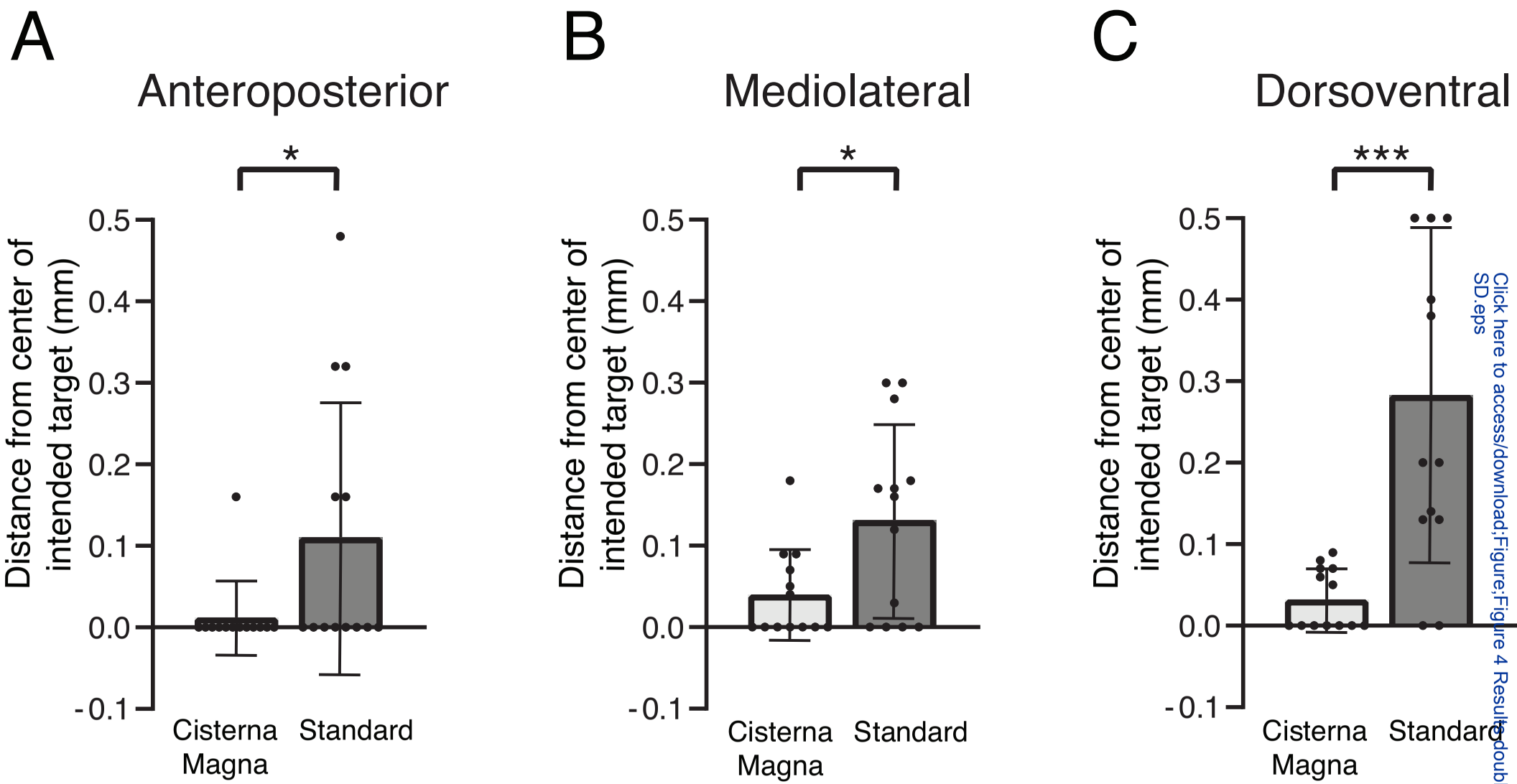

Table 1

	Standard stereotaxic approach*			Cisterna magna approach						
Region of interest	**Anterior Posterior** (Relative to Bregma)	**Mediolateral** (Relative to Bregma)	**Dorsoventral** (Relative to brain surface)	**Anterior Posterior** (Relative to Obex)	**Mediolateral** (Relative to brainstem midline)	**Dorsoventral** (Relative to brainstem surface)	**Strain**	**Genotype**	**Age**	**Sex**
Ventral respiratory group, caudal (cVRG)	NA (-8.3 to -7.5)	NA	NA	-0.7 to -1	1.3 to 1.5	-1.3	C57BL/6J & CD-1	WT	8-12 weeks	M&F
Ventral respiratory group, rostral (rVRG)	NA (-7.5 to 6.4)			-0.6 to -0.4	1.3 to 1.5	-1.5	C57BL/6J	WT	8-12 weeks	M
Medullary reticular nucleus, ventral part (MdV)	NA (-8.0)	NA	NA	-0.7 to -1	0.5 to 0.8	-1.3	C57BL/6J	vGluT2-ires-cre	10 weeks	M
Raphe obscurus (rostral pole)	NA (-7 to -8)	NA	NA	-0.4 to -0.8	0	-2.6 to -2.8	C57BL/6J	Sert-cre	2-9 months	M&F
Hypoglossal nucleus, caudal	NA (-7.6 to -7.9)	NA	NA	-0.2 to -0.4	0.1 to 0.15	0.7 to 0.9	C57BL/6J	ChAT-ires-cre	3-11 months	M&F
Hypoglossal nucleus, intermediate	(~) -7.0 to -7.1	0.15 to 0.25	-4.5 to -4.7	-0.1 to -0.2	0.1 to 0.15	1.0 to 1.2	C57BL/6J	ChAT-ires-cre, WT	3-11 months	M&F
Hypoglossal nucleus, rostral	-6.5 to -6.7	0.15 to 0.25	-4.4 to -4.5	0 to 0.2	0.15 to 0.2	1.2 to 1.4	C57BL/6J	ChAT-ires-cre	2-6 months	M&F
Intermediate reticular nucleus (Irt) parahypoglossal	(~) -6.8 to 7.0	1.2 to 1.3	-4.8	-0.2 to +0.2	1.2	1.3	C57BL/6J	ChAT-ires-cre, WT	2-10 months	M&F
Gigantocellular nucleus, ventral portion (GiV)	(~) -6.5 to -7.0	0.2 to 0.25	-5.2 to -5.4	-0.2 to -0.4	0.2 to 0.25	-2.75 to -2.85	C57BL/6J	vGaT-ires-cre, vGluT2-ires-cre	3-5 months	M&F
Gigantocellular nucleus, intermediate portion	-6.3 to -6.5	0.2 to 0.3	-4.7 to -4.9	-0.3 to 0	0.2 to 0.3	-2.45 to -2.65	C57BL/6J	vGaT-ires-cre, vGluT2-ires-cre	3-7 months	M&F
Raphe pallidus	-6.2 to -6.5	0	-5.6	-0.1 to -0.2	0.2	-2.9	C57BL/6J	vGaT-ires-cre, Sert-cre	2-11 months	M&F
Lateral paragigantocellular nucleus, LPGi	(~) -6.2 to -7.0	0.5 to 0.7	-5.6	-0.2 to -0.5	0.5	-2.9 to -3.0	C57BL/6J	vGaT-ires-cre, Sert-cre	2-7 months	M&F
Compact nucleus of the ambuus complex, cAmb	-6.2 to -6.5	1.3 to 1.5	-4.8	0 to -0.2	1.3 to 1.5	-2.5 to -2.6	C57BL/6J	WT	10 -16 weeks	M
(DPGi)	-6.0 to -6.3	0.15	-4.0 to -4.3	+0.1 to -0.1	0.15	-1.8	C57BL/6J	vGaT-ires-cre, vGluT2-ires-cre	3-7 months	M&F
Gigantocellular nucleus, proper (Gi)	-6.0 to -6.3	0.15	-4.5 to 5.0	+0.1 to -0.2	0.15	-2.15 to -2.4	C57BL/6J	vGaT-ires-cre, vGluT2-ires-cre	3-11 months	M&F
Gigantocellular nucleus, alpha (GiA)	-6.0 to -6.3	0.25 to 0.3	-5.2 to 5.4	+0.2 to -0.1	0.25 to 0.3	-2.65 to -2.75	C57BL/6J	vGaT-ires-cre, vGluT2-ires-cre	3-7 months	M&F
Intermediate reticular zone, (Irt) parafacial	-6.1 to -6.3	0.9 to 1.2	-5 to -5.2	+0.2 to 0.0	0.9 to 1.2	-2.15 to -2.3	C57BL/6J	ChAT-ires-cre	3-8 months	M&F
Raphe Magnus	-5.8 to -6.0	0	-5 to -5.2	+0.2 to -0.1	0	-2.6 to -2.8	C57BL/6J	Sert-cre, Pet1-flpe, Pet1-cre, vGaT-ires-cre	2-10 months	M&F

* Coordinates were derived from Paxinos mouse atlas and further optimized to reach verified target

(~) Cannot be reached consistently depending on age, sex and mouse strain

Table of materials

Dear Editor,

Thank you for your further insightful comments. We believe we addressed all your concerns in the updated manuscript and have listed our response below.

We look forward to hearing from you regarding our submission and to respond to any further questions and comments you may have.

Yours sincerely,

Krutika Joshi & Veronique Vanderhorst

Comment 1: Line 53-61. “Please provide references for this citing previously published studies.”
Response 1: We have added three references to the text- Paxinos and Franklin (2001), Popesko, et al (1992) and Allen Brain Atlas (2004) which demonstrate the anatomical shape of the cerebellum in relation to the brainstem, the slanted shape of the occipital bone and the presence of neck muscles covering the caudal portion of the occipital bone.

Comment 2: Line 303-313. “Please provide representative results for the data cited here. The results can either be in tabular form or graphs representing the data. We need results to show the effectiveness of the technique. Unpublished data cannot be cited. The JoVE publication can either serve as the primary publication for this data or the authors can wait for the parent publication to be out first and make JoVE as the child publication for this.”
Response 2: Thank you for your guidance. As instructed, we now represent the results of comparisons between the accuracy of the cisterna magna and standard approaches in three relevant planes in new Figure 4 and we have referenced Figure 4 in the ‘representative results’ section. The bar graphs with dot plots contain the data and the legend lists the summary of the t-statistics.

Comment 3: Line 381-384. “Please provide references for this citing previously published studies.”
Response 3: We have added existing references to the text related to burr hole technique (reference 1), anatomy of the skull and muscles (reference 6), and the distance between AP and DV zero points and target sites (2 and 7).